Distribution of Platinum Particles in the Bimodal Micropore System of Activated Carbon

by **György Onyestyák**

Institute of Surface Chemistry and Catalysis, Chemical Research Center, Hungarian Academy of Sciences, P. O. Box 17, H-1525 Budapest
(phone: +36-1-325-7900/403; fax: +36-1-325-7554; e-mail: ony@chemres.hu)

Platinum (Pt)/activated-carbon catalysts were prepared and characterized by pore-size distribution (PSD), propane-sorption dynamics, and activity of cyclohexane dehydrogenation to benzene. The batch-type frequency-response (FR) spectroscopic technique was applied to determine the mass-transport rate of propane sorption. Two parallel sorption processes of different time constants were distinguished, suggesting that adsorption proceeds in smaller and larger micropores that are not interconnected. Increasing Pt loading affected the propane mobility, but increased the dehydrogenation activity only up to *ca.* 1 wt-% of Pt content. It was concluded that clusters of metallic Pt-atoms are located preferentially at the narrowest pores. Blocking these micropores, the Pt reduces the carbon surface available for sorption; also, a significant fraction of the metal becomes inaccessible for the reactant.

Introduction. – Carbon materials are often used as support for metal catalysts because carbon can stabilize high metal dispersion without providing the catalyst with non-metallic activity [1]. The structure of the activated carbons or charcoals develops during the carbonization of a carbonaceous polymer material, followed by activation in a second step [2–6]. The obtained material is both chemically and structurally heterogeneous.

As inert catalyst support, carbon has the disadvantage that it is relatively difficult to anchor the active metal phase to its surface. It is, hence, difficult to generate and maintain a high-dispersion active phase on carbon. Metal dispersion can be dependent on the degree of support oxidation [7–9]. However, the best platinum (Pt) fixation was suggested to have been achieved when the catalyst particle generated hole in the support, wherein it uniquely fitted [10]. In activated carbons, the micropores may represent a physical barrier before the sintering process of the metal particles.

It was found in the reaction of heptane isomerization and aromatization [11] that the activity of Pt/activated-carbon catalysts was independent of the reduced Pt-atom concentration in the catalyst. Moreover, in the hydrogenation of olefins, *e.g.*, cyclohexene, some carbon-supported catalysts showed different activities at similar dispersions, or similar activities at different Pt dispersions [12]. At high dispersion, the metal particles could have been deposited at the narrow pores of the supports, rendering part of the metal surface inaccessible to the reactant. The possible activity loss due to pore blocking has long been recognized [13]. However, only a few works are known to give experimental verification to this phenomenon.

Recently, the frequency-response (FR) method was shown to be effective in the investigation of the mass-transport kinetics in various adsorbents [14]. In principle, this technique can be applied to distinguish the rate-governing step of a sorption mass-transport process and to determine the dynamic parameters of the process [15]. Results of FR examinations provided experimental evidence for the presence of non-interconnected micropores in the activated carbons by distinguishing two parallel diffusion processes with different time constants [16]. Correlation was found between the bi- and unimodal pore structures of activated carbon and carbon nanotube samples, respectively, and the equilibrium and dynamic-sorption behavior of the samples [17]. However the relation between the structural characteristics and the mass-transport properties of various carbon adsorbents is not fully understood yet.

The aim of this study is to learn more about the dynamic-sorption properties and the catalytic activity of Pt-loaded activated-carbon catalysts, taking advantage of the FR method, and by using the dehydrogenation of cyclohexane as a model reaction.

Experimental. – The granules (0.85–1.7 mm in size) of a commercial charcoal (*BDH Laboratory Supplies*, *Merck Ltd.*, UK) were ground and sieved. The fraction of size 0.71–0.50 mm was treated for 24 h with 2N HCl soln. at r.t. The ignition residue (ash) of the obtained carbon was less than 0.1 wt-%. The washed carbon was subjected to oxidation treatment with 5N HNO_3 soln. at 80° for 3 h to generate oxygen-containing surface groups, which can function as anchoring sites for Pt. The oxidized carbon was washed with hot dist. H_2O until the pH of the washing H_2O increased to 5. The material was dried overnight at 80°, and then used for loading with different salts. The support was impregnated with basic (pH 9) aq. $[Pt(NH_3)_4]Cl_2$ soln. (*Strem Chemicals)* as precursor to obtain a Pt content of *ca.* 1 or 5 wt-%. The wet samples were dried again overnight at 80°. The carbon-bound Pt complex was decomposed by heating the sample in an N_2 flow to 400° at a rate of 10°/min, keeping the sample at the final temp. for 1 h. Then, the samples were reduced *in situ* at 300° for 1 h under an H_2 flow in a catalytic reactor.

To prepare sodium (Na)/activated-carbon samples, having a metal content of up to *ca.* 7 wt-%, the oxidized carbon was impregnated with NaN_3, following the impregnation with drying procedure. Decomposition to Na metal and N_2 was carried out *in situ* in a frequency-response (FR) sample holder under ultra-high vacuum (UHV) and a temp. of 450°.

Nitrogen (N_2; 99.995% purity; *Messer Hungarogáz Kft.*, Hungary) was applied for measuring the isotherm for N_2 adsorption. Propane (99.95% purity; *Linde Gas*, UK) was selected to probe the dynamic-adsorption properties by the FR method. In the catalytic tests, cyclohexane (> 99%; *Interkémia Kft.*, Hungary) and H_2 (> 99.995%; *Messer Hungarogáz Kft.*, Hungary) were used. N_2-Adsorption isotherms were determined at −196° using a conventional all-glass BET system. Before the adsorption measurements, the samples were treated in a N_2 flow overnight at 300°, and degassed by evacuation for 1 h at the same temp. The Pt-containing samples were prereduced before the catalytic test.

The batch-type FR apparatus, which was used to study the mass-transport dynamics of propane sorption, was described previously [18]. The sample (*ca.* 200 mg) was distributed in a glass-wool plug placed in the FR chamber, and then degassed for 1 h under high vacuum at 300°. The sample was cooled to 100°, which was the selected temp. of the FR measurement, and equilibrated with adsorptive propane at a pressure in the range of 0.1–0.8 kPa. A ±1% square-wave modulation was applied on the volume of the FR chamber by different frequencies between 0.01 and 10 Hz. The generated response pressure-wave was recorded. Measurements were carried out under identical conditions, with and without adsorbent in the chamber. The equivalent fundamental sine waves were generated by *Fourier* transformation of the response pressure-waves. A response wave-function was defined by the phase lag and the amplitude ratio of the pressure waves. The FR spectrum was derived by plotting the in-phase (real) and out-of-phase (imaginary) components of the response wave-functions *vs.* the perturbation frequency.

Yasuda [15] generated theoretical FR spectra for different possible rate-controlling mechanisms of sorption mass-transport processes in porous solids, such as rate-controlling sorption on different sorption sites or rate-controlling diffusion in micropores. The dynamic parameters of the rate-controlling mass-

transport process were obtained from the experimental FR spectra as the parameters of the best-fit theoretical FR spectrum.

The Pt/carbon catalysts were prepared from the catalyst precursors by *in situ* reduction in a flow-through microreactor used for catalytic dehydrogenation of cyclohexane. The cyclohexane was fed in the reactor, having a bed volume of *ca.* 2 ml, by a piston pump (*Gilson Model 302*). The feed rate was *ca.* 1.2 ml h^{-1}. The catalyst was contacted simultaneously with H_2 at a flow of 0.05 mol h^{-1} and at a total pressure of 13 bar. The space velocity was 2.0 $g_{CH}\, g_{cat}^{-1}\, h^{-1}$, and the reaction temp. varied between 200 and 420°. The reactor effluent was analyzed by online GC measurement using a commercial fused-silica capillary column (*Supelco DH 100*) and a flame-ionization detector (FID).

Results and Discussion. – The N_2-adsorption isotherms were used to characterize the microporosity of the samples. The isotherms were of type I according to the BDDT classification. This type is characteristic for adsorption in microporous solids. Adsorption hysteresis was not observed, even at higher relative pressures (see isotherms in ref. [17]). What is important to notice is that the presence of Pt resulted in decreased N_2 uptake. However, the adsorption isotherms of the prereduced Pt/activated-carbon samples were overlapping in the range of 1 to 5 wt-% Pt content.

The N_2-adsorption isotherms could be described by the two-term *Dubinin–Radushkevich* (DR) relationship (*Eqn. 1*), substantiating that the micropores represent two distinct size ranges [19]:

$$W = W_1 + W_2 = W_{01} \cdot \exp[(\{-RT/\beta E_1\} \cdot \ln(p_0/p))^2] + W_{02} \cdot \exp[(\{-RT/\beta E_2\} \cdot \ln(p_0/p))^2] \quad (1)$$

In *Eqn. 1*, E is the so-called characteristic energy of adsorption, β is the affinity coefficient, W is the volume of quantity adsorbed at relative pressure p_0/p and temperature T, filling micropores, and W_0 is the total, limiting micropore volume. The parameters, related to the pores in a distinct size range, are indicated either with subscripts 1 or 2. For N_2, a β value of 0.33 was assumed [20][21]. Selected examples (*Table 1*) for micropore volumes and characteristic adsorption energies were obtained for the parameters of *Eqn. 1*, giving the best fit to the N_2-adsorption isotherms.

Table 1. *Micropore Volumes and Characteristic Adsorption Energies from* Dubinin–Radushkevich *Analysis of N_2-Adsorption Isotherms.* For details, see *Exper. Part* and *Eqn. 1.*

Sample	Absorption volume [ml/g]		Adsorption energy [kJ/mol]	
	W_{01}	W_{02}	E_1	E_2
Oxidized *BDH* carbon	0.28 ± 0.003	0.14 ± 0.003	21.7 ± 0.86	5.8 ± 0.22
20 wt-% NaN_3/*BDH* carbon	0.15 ± 0.003	0.05 ± 0.003	25.2 ± 1.38	7.7 ± 0.53
1 wt-% Pt/*BDH* carbon	0.21 ± 0.003	0.14 ± 0.003	22.1 ± 0.79	5.8 ± 0.12

The data in *Table 1* show the influence of loading on the micropore volume accessible for adsorption. Loading of salts as metal sources, *e.g.*, $[Pt(NH_3)_4]Cl_2$ or NaN_3, decreased both kinds of micropore volumes. Characteristic adsorption energies increased significantly. Formation of Pt metal in the concentration range used in practical catalytic applications resulted in a significant decrease only in the narrower

micropores, reflecting the preferred location of the catalytically active metal clusters. Pore-size distributions were calculated by the semi-empirical *Spitzer* method, using the results of the above DR analysis (data not shown) [22]. The distribution curves were resolved into two component peaks. The most-frequent slit widths were either about two or three times the distance between two graphene layers in the graphite crystal, *i.e.*, *ca*. 0.64 nm and 0.92 nm, respectively.

The intensity decrease of the narrower pore peak showed significant selectivity to capture Pt nanoparticles, as suggested by the significant drop of the free volume on Pt introduction (*Table 1*). (Salts, *e.g.*, NaN_3 or $[Pt(NH_3)_4]Cl_2$ precursor can be fixed on both pore grades). As the N_2-adsorption isotherms of the prereduced Pt/activated-carbon samples were about the same for Pt contents of 1 *vs.* 5 wt-%, the calculated pore-size distributions were, consequently, found to be not too different. It can be concluded that Pt clusters, formed at the entrance of the narrower micropores, completely block a great part of those, and a further increase of the metal-cluster size in this concentration range has no significant influence for the accessible carbon or metal surfaces.

Different FR spectra, as shown in the *Figure*, demonstrate the differences of propane-sorption dynamics in variously treated activated-carbon samples. When the characteristic time of periodic modulation approaches the time constant of the studied transport process, resonance occurs, as indicated by the appearance of a step and a peak in the FR spectra with the real and imaginary parts of the complex function, respectively. Theoretical FR functions can be determined for isothermal transport in uniform particles [15][23]. When diffusion is rate-determining, the in-phase and out-of-phase curves approach each other asymptotically at higher frequencies. The best computer fits of the responses in *Figure*, recorded with propane, can only be described by such bimodal characteristics, *i.e.*, two independent diffusion-controlled processes.

The main unique advantage of the FR technique is its ability to distinguish different molecular mobilities, parallel mass-transport processes. If the wider micropores were transport pores feeding the smaller pores, the transport rate would be given by the only one process having the lower time constant. The bimodal size distribution of the micropores and the bimodal character of the FR spectra reflecting intraparticle diffusion suggest that the smaller and the larger micropores of the activated carbon are not interconnected, *i.e.*, graphite nanocrystallites in this activated carbon from an anisotropic pore system with two types of independent paths for propane transport (see details in [16]).

The adsorption of the non-polar propane and, conceivably, its transport, are controlled by the mobility of the molecules close to the adsorption equilibrium. Thus, the characteristics of the sorption mass transport are related to the energy of adsorption. Different intensity ratios of the decomposed component FR functions (*Figure*, dotted and dashed lines) were observed for the various samples. According to theory, the intensity of each of these response signals is determined by the sorption capacity associated with each of these two diffusion processes. The total FR intensity is proportional to the gradient of the adsorption isotherm at the equilibrium pressure of the measurement.

The FR spectra shown in the *Figure* suggest that the introduction of metal compounds into porous carbon significantly modifies the mass-transport properties of

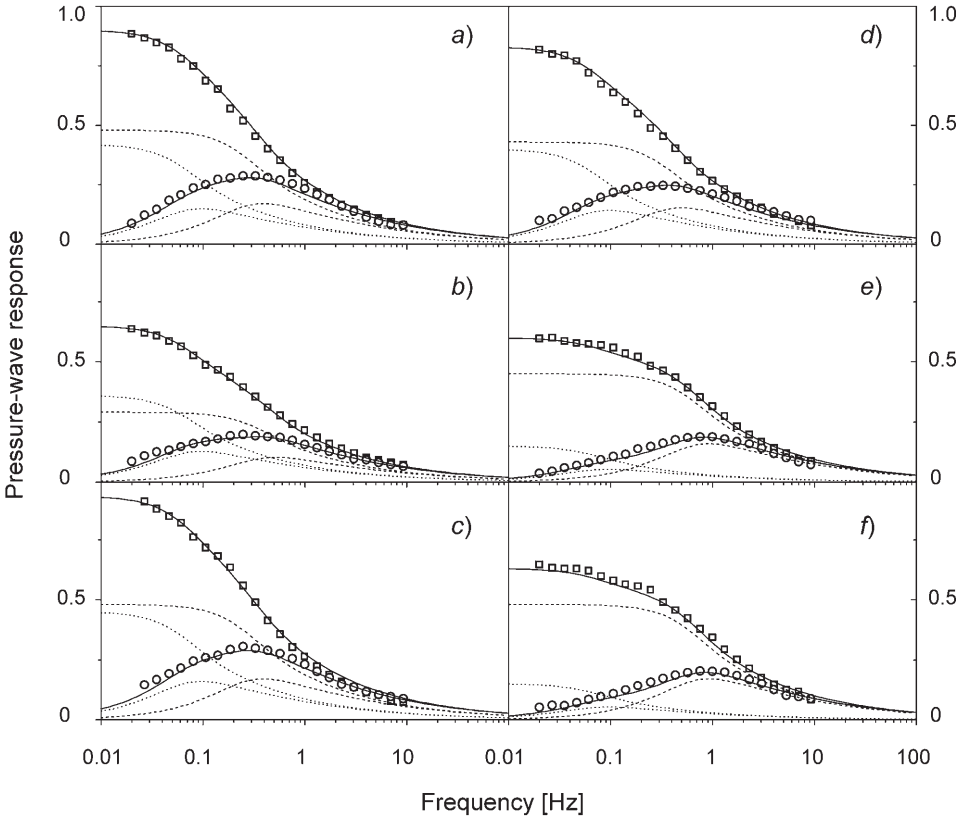

Figure. *Frequency-response spectra recorded for the adsorption of propane on 200 mg of* BDH *adsorbent at 133 Pa and 100°*. Symbols correspond to the in-phase (□) and out-of-phase components (○) of the experimental response functions. Full, dashed, and dotted lines represent the best-fit characteristic FR spectra and its components, derived using the model developed by *Yasuda* [15] for rate-controlling isothermal diffusion in uniform, spherical particles in a bidisperse micropore system. *a*) Oxidized *BDH* carbon support; *b*) 20 wt-% NaN_3/*BDH* carbon, prepared by impregnating with NaN_3; *c*) after decomposition of NaN_3 at 450° under UHV for 5 min. Spectra were obtained for 1 wt-% Pt/*BDH* carbon after *d*) impregnation of the *BDH* carbon with $[Pt(NH_3)_4]Cl_2$ solution and drying; after *e*) decomposition of the carbon-bound Pt complex at 400° under N_2; and *f*) followed by reduction of the sample in a H_2 flow at 300°.

the support. In the *Figure* (panel *a*), the propane FR spectrum of the oxidized sample, *i.e.*, the *BDH*-type activated carbon, is shown after acid treatment with HCl and HNO_3. This spectrum can be compared to the spectra recorded on the same support after different loadings or treatments. The impregnation with NaN_3 up to 20 wt-% gave rise to a great decrease in the total FR intensity (panel *b*). Both component steps and peaks of this FR spectrum had lower heights; however the intensity of the high-frequency signal, which can be assigned to faster intracrystalline diffusion in the wider pores, decreased to a greater extent than the signal intensity for the slower diffusion in the narrower micropores. This finding shows a good correlation of static adsorption results,

where a greater volume decrease of wider micropores was detected in the pore-size distribution.

NaN_3 was used as a source of Na metal to form different clusters for easier characterization of the various sites in the activated carbon, compared to the more difficult case of Pt. It was found to be fully decomposed by heat treatment for 5 min in the FR sample chamber at 450° under ultra-high vacuum (UHV), with no change up to 400°. However, the original FR spectrum was again observed (compare panels *a* and *c* in the *Figure*) without any influence of the presence of the Na clusters. Na Vapor was found to be highly volatile, and a Na mirror was formed on the unheated walls of the apparatus. The study of Na clusters in the *BDH*-type activated carbon, having low intercrystalline diffusion resistance, and without entrapment was unsuccessful.

In panel *d* of the *Figure*, significantly lower intensities of FR signals were recorded after impregnation with $[Pt(NH_3)_4]Cl_2$, compared with the support sample (panel *a*). The relatively low metal (*i.e.*, metal-complex) content resulted in a significant decrease in the intensity of both FR peaks. Decomposition of the Pt complex in N_2 flow at 400° to platinum oxide species resulted in a great decrease of the low-frequency peak, which can be assigned to a slower propane-transport process in the narrower slits (*Figure*, panel *e*). The same FR spectrum obtained after reduction of the oxide was formed in H_2 flow at 300° (*Figure*, panel *f*). The total FR-intensity decrease of the spectra recorded for the oxidized or reduced forms was similar to those obtained with the high-amount NaN_3 impregnation. However, the ratio of the spectral components reflecting the different change of parallel mass-transport processes was completely different. The Pt-containing particles were placed at the mouth of the narrower micropores already during the decomposition of the Pt precursor. Although the concentration of the Pt species was much less than for the NaN_3, blocking of a part of the narrower pores resulted in the 'elimination' of a great part of the microporous surface, which, thus, resulted in the low-frequency FR signal.

Surprisingly, the formation of Pt-metal nanoparticles upon reductive treatment resulted in almost the same spectra, which suggests that the size and location of the pure Pt-metal cluster was nearly the same as for the precursor oxide particles. Increasing the Pt content from 1 to 5 wt-% had no influence on the FR spectra, indicating that there is no difference in the propane-sorption dynamics when the Pt cluster can form bigger plugs at the narrow pores. The results of both static- and dynamic-sorption measurements were found to be well-correlated.

The product distributions shown in *Table 2* reflect the changes of activity and selectivity during the conversion of cyclohexane on loaded and unloaded activated-carbon catalysts, applying different Pt concentrations at increasing temperature in the range 300–420°. The parent oxidized activated-carbon support formed only trace amounts of the desired benzene, giving a practically inert support in a wide temperature window, in spite of the acid pretreatments. The position of the thermodynamic equilibrium of the dehydrogenation of cyclohexane to benzene, above *ca.* 350°, was completely on the side of the aromatic product after a relatively narrow temperature interval of shift (*ca.* 120°). Although the activated carbon was treated with two different types of acid (HCl and HNO_3), the support applied had very low activity. Beside benzene by-products, formed by skeletal isomerization of cyclohexane, methylcyclopentane and hexane isomers were also produced. Surprisingly the amount

Table 2. *Temperature-Dependent Product Distribution* (in wt-%) *for the Dehydrogenation of Cyclohexane to Benzene* (Main Reaction) *over Commercial and Pt-Loaded Activated-Carbon Catalysts*

Pt Content [%]	Product	Temperature [°]								
		300	320	340	360	380	390	400	410	420
0	Cyclohexane[a])	99.2	98.8	97.9	97.2	96.2	96.0	95.6	95.0	94.8
	Hexanes	0.04	0.04	0.04	0.04	0.14	0.19	0.30	0.30	0.33
	Methylcyclopentane	0.52	1.00	1.71	2.30	2.72	2.94	2.94	3.08	2.96
	Benzene	0.1	0.1	0.1	0.2	0.4	0.5	0.7	1.0	1.1
1	Cyclohexane[a])	99.5	98.7	97.3	94.5	85.9	77.6	67.0	54.9	41.9
	Hexanes	0.03	0.03	0.03	0.05	0.21	0.24	0.30	0.37	0.40
	Methylcyclopentane	0.38	1.05	1.74	2.37	3.02	3.12	3.11	3.20	3.14
	Benzene	0.1	0.3	1.0	3.0	10.8	18.8	29.1	41.1	54.0
5	Cyclohexane[a])	99.5	99.1	98.1	95.5	88.0	80.4	70.6	56.6	44.3
	Hexanes	0.05	0.03	0.04	0.11	0.15	0.36	0.39	0.45	0.50
	Methylcyclopentane	0.32	0.68	1.12	1.70	2.28	2.69	2.91	2.99	3.02
	Benzene	0.1	0.2	0.8	2.7	9.4	16.5	25.9	39.6	51.7

[a]) Unreacted starting material.

of these by-products hardly changed between 390 and 420°, where benzene production increased in the highest degree; also, their yields were the same for all three catalyst samples.

From the above data, it can be concluded that acid treatment does not generate strong enough acidic sites, although these, as functional groups, can play an important role in anchoring of impregnated species. The introduction of highly dispersed Pt metal resulted in increasing production of benzene upon rising the reaction temperature. The benzene yield increased nearly linearly with temperature above 390°, and a good selectivity was maintained, with only minute by-product formation.

It is a striking phenomenon that the benzene yield did not depend on the Pt content (in the range 1–5%), a finding that was well-correlated with the FR results. This, therefore, cannot express any change of the accessibility of platinum clusters or higher active surface of the Pt metal. It seems that Pt clusters are hidden partly at the entrances of the narrower micropores existing in the graphite crystallites and building up the macroporous structure of the activated carbon; so, only a small surface at the pore mouth is probably available for the reactant.

The bimodal micropore-size distribution and the character of the bimodal sorption kinetics reflected by the FR spectra suggest that the smaller and the larger micropores of the studied activated carbon are not interconnected. Different changes in the extent of two parallel micropore-diffusion processes with different time constants, as distinguished in the FR-rate spectra, indicate a significant effect of loading. In activated carbons, the microporosity responsible for the high surface area may act as a physical barrier to the metal particles deposited, resulting in resistance to sintering [13]. This is attributed to deposition of metal particles of high dispersion at the narrowest pores of the support, which renders part of the metal surface inaccessible to the organic substrates. Such a blocking effect found for Pt catalysts on activated-carbon support containing small micropores is possible. The possibility of the loss of a great part of the

catalytically active surface area due to blocking has long been recognized. However, there have been only few verified examples of this phenomenon so far. The present results, thus, clearly support this hypothesis.

Financial support by the *Hungarian Research Fund* (OTKA T 037 681) and the *National Office for Research and Technology* (GVOP-3.2.1.-20004-04-0277/3.0) is kindly acknowledged. I would like to thank Prof. *Lovat V. C. Rees* and Prof. *József Valyon* for helpful discussion, Mrs. *Ágnes Wellisch* for her excellent technical assistance, and Dr. *Attila Bóta* for calculating the pore-size distributions.

REFERENCES

[1] F. Rodriguez-Reinoso, *Carbon* **1998**, *36*, 159.
[2] R. C. Bansal, J. B. Donnet, F. Stoeckli, 'Active Carbon', Marcel Dekker, New York, 1988.
[3] B. E. Warren, *Phys. Rev.* **1941**, *59*, 693.
[4] N. Setoyama, M. Ruike, T. Kasu, T. Suzuki, *Langmuir* **1993**, *9*, 2612.
[5] K. Kaneko, C. Ishii, M. Ruike, H. Kuwabara, *Carbon* **1992**, *30*, 1075.
[6] T. Wigmans, *Carbon* **1989**, *27*, 13.
[7] F. Coloma, A. Sepulveda-Escribano, J. L. G. Fierro, F. Rodriguez-Reinoso, *Appl. Catal. A* **1997**, *150*, 165.
[8] M. A. Fraga, E. Jordano, M. J. Mendes, M. M. A. Freitas, J. L. Faria, J. L. Figueiredo, *J. Catal.* **2002**, *209*, 355.
[9] A. Erhan Aksoylu, M. Madalena, A. Freitas, M. Fernando, R. Pereira, J. L. Figueiredo, *Carbon* **2001**, *39*, 175.
[10] R. T. K. Baker, E. B. Prestridge, R. L. Garten, *J. Catal.* **1979**, *56*, 390.
[11] I. Rodriguez-Ramos, A. Guerrero-Ruiz, *Appl. Catal. A* **1994**, *119*, 271.
[12] L. B. Okhlopkova, A. S. Lisitsyn, V. A. Likholobov, M. Gurrath, H. P. Boehm, *Appl. Catal. A* **2000**, *204*, 229.
[13] L. R. Radovic, F. Rodriguez-Reinoso, in 'Chemistry and Physics of Carbon', Ed. P. A. Thorwer, Marcel Dekker, New York, 1997, Vol. 25, pp. 243–358.
[14] G. Onyestyák, L. V. C. Rees, *J. Phys. Chem. B* **1999**, *103*, 7469.
[15] Y. Yasuda, *Heterogen. Chem. Rev.* **1994**, *1*, 103.
[16] G. Onyestyák, J. Valyon, A. Bóta, L. V. C. Rees, *Helv. Chim. Acta* **2002**, *85*, 2463.
[17] G. Onyestyák, J. Valyon, K. Hernádi, I. Kiricsi, L. V. C. Rees, *Carbon* **2003**, *41*, 1241.
[18] L. V. C. Rees, D. Shen, *Gas Sep. Purif.* **1993**, *7*, 83.
[19] T. I. Izotova, M. M. Dubinin, *Zh. Fiz. Khim.* **1965**, *39*, 2796.
[20] J. Garrido, A. Linares-Solano, J. M. Martin-Martinez, M. Molina-Sabio, F. Rodriguez-Reinoso, R. Torregrosa, *Langmuir* **1987**, *3*, 76.
[21] F. Ehrburger-Dolle, M. Holz, J. Lahaye, *Pure Appl. Chem* **1993**, *65*, 2223.
[22] Z. Spitzer, V. Bíba, O. Kadlec, *Carbon* **1976**, 14, 151.
[23] R. G. Jordi, D. D. Do, *Chem. Eng. Sci.* **1993**, *48*, 1103.

Received February 8, 2007